MAGNETIC RESONANCE IN CHEMISTRY
Magn. Reson. Chem. **36**, S135–S144 (1998)

Solid-state ^{13}C chemical shift tensors in terpenes

Part I. Spectroscopic methods and chemical shift structure correlations in caryophyllene oxide†

James K. Harper, Gary McGeorge and David M. Grant*

Department of Chemistry, University of Utah, Salt Lake City, Utah 84112, USA

Received 19 December 1997; revised 6 February 1998; accepted 6 February 1998

ABSTRACT: Principal values of the ^{13}C chemical shift tensor were obtained for the 15 carbons of solid caryophyllene oxide using an improved PHORMAT NMR analysis. The improvements include TIGER processing and improved proton decoupling. TIGER is an alternative to Fourier methods and shortens 2D data collection by incorporating information from a high-resolution isotropic 1D FID to allow accurate processing of even severely truncated 2D evolution FIDs. In caryophyllene oxide, data collection required less than 1 day, giving significant time savings over comparable 2D Fourier methods. Experimental principal values were assigned with high statistical confidence to specific carbons by comparing them with corresponding calculated values. Correctly assigned values were used to evaluate five different tensor calculation methods. For caryophyllene oxide, the B3PW91 method gave the best correlation with experimental principal values with an RMS error of 2.3 ppm. Refinement of x-ray positions for hydrogens was shown to improve the calculated RMS error by a factor of >2. Calculated tensors can be used to provide principal value orientations in the three methyl groups of caryophyllene oxide. One of the perpendicular component, $\delta_\perp$, is found to exhibit the largest shift variation and dominates the methyl shifts. Sterically unfavorable non-bonded interactions between proximate hydrogens are shown to correlate with this large upfield shift in the $\delta_\perp$ component. © 1998 John Wiley & Sons, Ltd.

KEYWORDS: NMR; ^{13}C NMR; PHORMAT; chemical shift tensors; terpene; caryophyllene oxide

INTRODUCTION

For many years, NMR spectroscopy has provided structurally sensitive information. Usually the focus has been on relating isotropic liquid shifts to structural features. Emphasis on isotropic shifts, however, provides only one value per nucleus (i.e. one third of the trace of the chemical shift tensor). Actually, the mathematical expression which best describes the complete chemical shift interaction is a symmetrical second-rank tensor with six potentially observable values.[1] Isotropic shifts thus neglect useful structural information found in the tensor. Recently, a variety of solid-state NMR experiments have been developed which allow for measurement of these individual tensor components in both single-crystal and powdered solids.[2] These measurements depend upon solid samples where the rapid averaging of molecular orientation found in liquids is eliminated. For powdered samples, as emphasized in this work, only the three diagonalized tensor components may be observed directly. These tensor principal values are designated from high to low frequency by δ_{11}, δ_{22} and δ_{33}. The 2D phase corrected magic angle turning (PHORMAT) experiment is one of the most powerful new methods for obtaining principal shifts in powdered solids.[3] This technique, in a single experiment, provides principal values from the acquisition dimension for all carbons observable as isotropic peaks in the evolution dimension. In addition, no isotope labeling is required and the experiment can be carried out on standard equipment. However, PHORMAT's relatively low signal-to-noise ratio (S/N) and long acquisition times have precluded the method's use in routine analysis.

Two improvements have been introduced recently into the PHORMAT experiment, providing for a significant savings in total analysis time. The first is a processing technique known as the technique for importing greater evolution resolution (TIGER).[4] TIGER replaces Fourier transformation of the evolution dimension with a linear model created from a high-resolution 1D FID. Applying the TIGER model to the 2D FID then directly extracts constant evolution frequency responses equivalent to the slices that could be separated by Fourier transforming an FID with many more evolution increments. Thus, high resolution in the evolution dimension is achieved without acquiring an extensive evolution FID. In both TIGER and Fourier-processed PHORMAT datasets, the acquisition dimension is treated the same. The second improvement is the inclusion of a two-pulse phase-modulation (TPPM) in the

* *Correspondence to*: D. M. Grant, Department of Chemistry, University of Utah, Salt Lake City, Utah 84112, USA.
† Dedicated to Professor John D. Roberts on the occasion of his 80th birthday.
Contract/grant sponsor: National Institutes of Health; *Contract/grant number*: GM 08521-28.

CCC 0749-1581/98/SI0135–10 $17.50

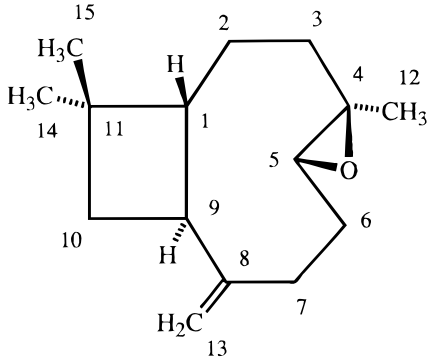

Figure 1. Structure of caryophyllene oxide.

^{13}C–$\{^1H\}$ decoupling[5] during the PHORMAT pulse sequence. The improved decoupling results in significantly narrower isotropic lines and corresponding greater peak heights for the same noise, thereby further reducing the total analysis time. Used together, the TIGER and TPPM techniques allow for rapid and accurate PHORMAT analysis of relatively large molecules.

We report here the application of the TIGER/TPPM modifications to the 2D PHORMAT of caryophyllene oxide (Fig. 1). This terpene contains carbons with a diverse variety of tensors, thus providing a rigorous test of the modified PHORMAT analysis. Tensor principal values for all carbons in caryophyllene oxide are reported. The time savings provided by TIGER analysis of PHORMAT data from caryophyllene oxide are outlined. An evaluation is given of TPPM linewidth improvements. The principal values for caryophyllene oxide are demonstrated to provide a foundation for both a rigorous assignment of solid-state isotropic shifts based on comparison with calculated principal values and for evaluation of various tensor computational methodologies. Finally, a description is given of how calculated principal values allow corresponding shift values to be oriented in the molecular frame. The structural implications of such three dimensional information are illustrated for the methyl carbons.

RESULTS AND DISCUSSION

TIGER and TPPM modifications to PHORMAT

In evaluating multi-dimensional NMR experiments, the time required for data collection is a key consideration. Routine experiments which suffer from long acquisition times are difficult to justify when more efficient alternatives exist. Therefore, the initial focus in this PHORMAT analysis of caryophyllene oxide was on evaluating the improvements in time efficiency provided by TIGER processing and TPPM decoupling.

The time savings realized from TIGER processing arise from the relatively small number of evolution dimension data points needed to resolve signals in the isotropic dimension.[4] Unfortunately, Fourier transformation of such a truncated dataset results in large sinc oscillations which severely degrade the extracted powder patterns in PHORMAT analysis. This severe truncation of the evolution dimension, however, does not have a corresponding drawback in the TIGER processing scheme. The collection of a truncated dataset enhances the S/N per unit time, as the shorter evolution times with less relaxation provide significantly higher S/N data. A more complete discussion of these issues is given elsewhere.[4]

PHORMAT data for caryophyllene oxide were collected and TIGER processed to determine the minimum time required for a successful analysis. Two separate datasets were collected, one with high resolution but low signal averaging per evolution increment suited to the closely spaced aliphatic carbons, while the second set emphasized S/N but reduced resolution for the well separated olefinic carbons. Acquisition of both datasets required only 21.3 h (i.e. 5.7 and 15.6 h, respectively, for the sp^2 and sp^3 optimized data) and provided high-quality powder patterns for all carbons. Comparable analyses performed in our laboratory without the advantages of TIGER processing have typically required 2–4 times longer.[4]

The additional benefit of running the analysis in 21.3 h as two separate experiments provided a 2.9 factor in the time savings over a single TIGER analysis of sufficient S/N (estimated to take 62.6 h) to observe simultaneously both sp^2 and sp^3 carbons. Thus, the judicious design of PHORMAT experiments can yield even greater time savings. Since sp^2 carbons are typically found to have much larger anisotropies than sp^3 carbons, the two-experiment approach outlined here should have general application in PHORMAT analyses whenever the olefinic or aromatic regions are well resolved relative to the aliphatic region.

The TPPM proton decoupling provides further time savings in PHORMAT analyses by providing greater ^{13}C signal intensity for a given number of scans. Analysis of the PHORMAT spectrum of caryophyllene oxide indicates that the methylene carbons, which are the hardest to decouple, are narrowed by about 42% compared with continuous wave decoupling. The higher S/N in methylene groups arising from the narrowing results in significant time savings compared with conventional decoupling. Other carbon (i.e. CH_3, CH and quaternary carbons) lines were narrowed to a smaller extent. When the S/N benefits of the TPPM/TIGER modifications are combined in dual experiments optimized to sp^2 and sp^3 carbons, the overall time saving is enhanced by nearly an order of magnitude.

A particularly clear example of the benefits of TIGER/TPPM is found in the separation of individual powder patterns for carbons 2 and 7. These carbons differ by only 0.4 ppm in their isotropic frequencies, yet the analysis clearly provides distinct patterns for each peak, as shown in Fig. 2. Such resolution is not possible from the truncated PHORMAT without TIGER, as seen by examining the PHORMAT isotropic projection shown in Fig. 3. However, the TIGER processing

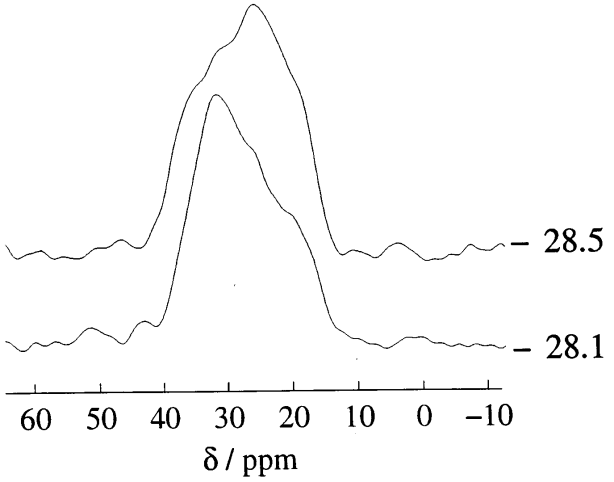

Figure 2. Powder patterns obtained for carbons 2 and 7 using TIGER processing of a 15.6 h PHORMAT spectrum. The carbons differ by only 0.4 ppm in the isotropic dimension, yet the two tensor powder patterns are clearly distinguishable using the methods described.

incorporates the high resolution from the isotropic spectrum shown, to differentiate easily the two powder patterns.

Overall, the use of TPPM decoupling and TIGER processing in the PHORMAT analysis provided high-quality principal values in two optimal experiments requiring less than 1 day on a moderately large molecule at natural abundance. Five additional representative examples of typical powder patterns and fits are shown in Fig. 4 for a third of the 15 carbons to illustrate the overall spectroscopic quality of these results.

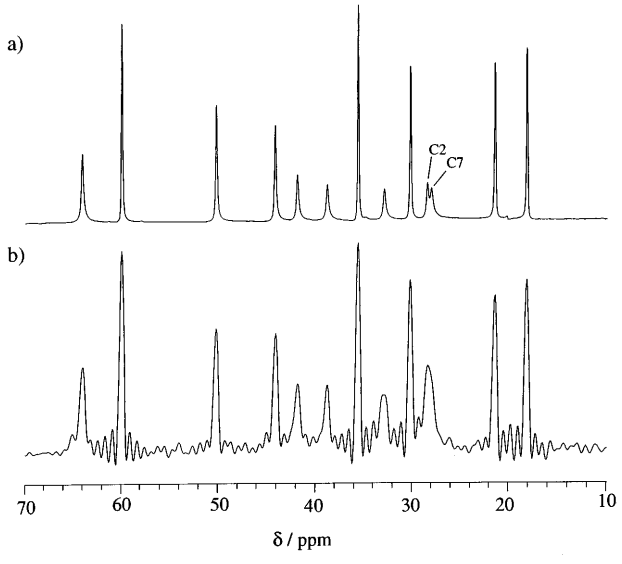

Figure 3. A PHORMAT isotropic projection (b) showing the poor resolution of carbons 2 and 7 obtained by Fourier transformation of the truncated 15.6 h PHORMAT spectrum. The top spectrum (a) shows the high-resolution isotropic spectrum from which the TIGER model was derived. As the peaks for carbons 2 and 7 are resolved here, TIGER incorporates this information in processing the 2D data, hence distinct powder patterns are obtained for the separate carbons.

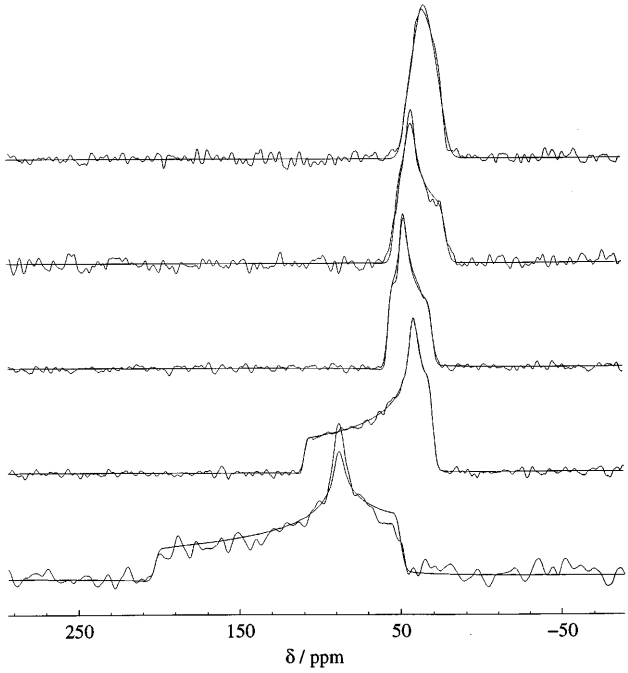

Figure 4. Typical powder patterns provided by TIGER processing of PHORMAT data. The fit to each pattern is drawn superimposed to illustrate the quality of fit commonly achieved. The included powder patterns are taken from carbons 6,3,1,4 and 13 (from top to bottom).

Solid-state ^{13}C shifts and their assignments

Experimental and theoretical principal shift values for caryophyllene oxide are given in Table 1. The B3PW91 theoretical results appear in parentheses alongside the corresponding experimental values.

Accurate characterization of all ^{13}C principal values in an organic molecule provides additional data for assigning the various resonances to specific carbons. Solid-state isotropic shift assignments can be difficult because of the lack of precedents in their use. At present they are often made by comparison with solution isotropic assignments,[6] the use of solid-state spectral editing sequences[7] or by comparison with *ab initio* calculated shifts.[6,8] The ability of PHORMAT to provide a large number of principal values in moderate-sized molecules free from magnetic susceptibility diversities will greatly aid in establishing future precedents for signal assignments based on principal values. In the meantime, the accuracy of modern shift tensor calculations has improved to the point that comparison of calculated and experimental principal values offers one of the best methods of peak assignment. Shift assignments based on the three principal values have the advantage that multiple comparisons per carbon are possible. This redundancy provides a means of resolving ambiguities which may arise by using only a single value as in the case of isotropic shifts.

All tensor comparisons were performed using root mean squared (RMS) distances between pairs of tensors

Table 1. Principal values for caryophyllene oxide and corresponding theoretical values.

Carbon	Chemical shift (ppm): Experiment (theory[a])			
	δ_{11}	δ_{22}	δ_{33}	$\delta_{average}$[b]
1	56.8 (59.4)	46.3 (48.2)	29.4 (31.1)	44.2 (46.2)
2	37.3 (40.6)	31.4 (33.3)	16.2 (15.2)	28.3 (29.7)
3	51.9 (54.2)	41.4 (42.6)	20.5 (22.8)	37.9 (39.9)
4	110.2 (109.2)	40.9 (39.2)	29.4 (31.0)	60.1 (59.8)
5	106.3 (105.5)	53.2 (58.6)	30.9 (35.0)	63.5 (66.4)
6	44.6 (45.2)	32.6 (35.4)	21.5 (21.8)	32.9 (34.1)
7	39.8 (42.1)	26.5 (27.0)	16.6 (17.5)	27.6 (28.8)
8	267.9 (266.0)	159.7 (158.1)	35.4 (29.2)	154.3 (151.1)
9	70.7 (69.9)	48.0 (48.6)	32.3 (32.8)	50.3 (50.5)
10	57.8 (59.6)	47.6 (47.7)	20.5 (16.4)	42.0 (41.2)
11	48.0 (46.5)	34.5 (32.9)	24.5 (24.2)	35.7 (34.5)
12	26.5 (27.4)	26.3 (24.6)	2.4 (2.4)	18.4 (18.1)
13	202.6 (205.9)	88.2 (85.4)	52.4 (42.0)	114.4 (111.1)
14	33.5 (33.5)	26.6 (27.7)	4.6 (1.4)	21.5 (20.9)
15	51.2 (54.2)	33.7 (33.2)	5.8 (−0.3)	30.2 (29.0)

[a] Theoretical tensor values, given in parentheses, calculated using the B3PW91 method and 6–31+G (2d, p) basis set. The structure used consisted of x-ray positions for heavy atoms and B3LYP/6–31G** refined hydrogen positions.
[b] Isotropic values were computed from the average of the fitted experimental principal values and vary slightly from the more accurate CP/MAS determined isotropic shifts.

rather than RMS deviation computed solely from the differences in the principal shift values. The distance between two tensors is defined as a surface integral of the differences of all points in an ellipsoidal representation of a tensor, not merely the three points characterizing the principal shift values. This important distinction between RMS distances and RMS differences has been treated both conceptually and mathematically by Alderman *et al.*[9]

Shift assignments for caryophyllene oxide were made by considering, as potentially correct assignments, all theoretical values within $\pm 2\sigma$ (± 4.6 ppm) of the experimental principal values. The assignments were done in a stepwise fashion. First, potential theoretical matches to δ_{11} were determined for all carbons. Nine carbons had multiple potential matches based on this single criterion. Ambiguous assignments were then further reduced by performing the same evaluation using the δ_{22} and finally the δ_{33} components; these are summarized in Table 2 (correct assignments are shown in bold). The importance of using all three parameters for comparison is clear, as inclusion of each additional

Table 2. Chemical shift assignments for solid caryophyllene oxide

Carbon	Theoretical matches to specific carbons[a,b]			
	δ_{11} only	δ_{11} and δ_{22}	δ_{11}, δ_{22} and δ_{33}	δ_{iso}
1	**1**, 3, 10, 15	**1**, 3, 10	**1**	**1**, 3, 10
2	**2**, 14	**2**, 14	**2**	**2**, 7, 15
3	**3**, 15	**3**	**3**	**3**, 10, 11
4	**4**	**4**	**4**	**4**
5	4, **5**	**5**	**5**	4, **5**
6	2, **6**, 7, 11	2, **6**, 11	**6**, 11	2, **6**, 7, 11, 15
7	2, **7**	**7**	**7**	2, **7**, 15
8	**8**	**8**	**8**	**8**
9	**9**	**9**	**9**	1, **9**
10	1, 3, **10**, 15	1, **10**	**10**	1, 3, **10**
11	6, **11**	6, **11**	6, **11**	3, 6, **11**
12	**12**	**12**	**12**	**12**, 14
13	**13**	**13**	**13**	**13**
14	**14**	**14**	**14**	12, **14**
15	3, **15**	**15**	**15**	2, 6, 7, 11, **15**

[a] Both experimental and theoretical values are taken from Table 1.
[b] Theoretical parameters within $\pm 2\sigma$ of the corresponding experimental values are considered possible matches. Final assignments are shown in bold.

parameter further reduces the number of ambiguous assignments. Unfortunately, even comparison using all principal values fails to distinguish clearly positions 6 and 11. However, C-6 is a methylene carbon whereas C-11 is non-protonated carbon. The difficulty in decoupling methylene carbons identifies the resonance at 32.9 ppm clearly as carbon 6 and the order in Table 2 reflects these independent data. For comparison, potential assignments from only isotropic shifts are also included in Table 2. Here unequivocal shift assignment can be made only for carbons 4, 8 and 13 based upon the $\pm 2\sigma$ agreement between experimental and theoretical isotropic shifts.

These data support the position that carbons may be reliably assigned using calculations of reasonable accuracy. It should be emphasized, however, that the confidence with which assignments can be made depends on the accuracy of the calculated principal values. This approach presumes that errors in experimental principal value (± 0.7 ppm) are sufficiently smaller than the theoretical range of $\pm 2\sigma$ (about 4.6 ppm) so that the range actually represents the region in which the experimental shift component must be found. This illustrates the importance of using the best tensor calculation procedure available (see the next section) and clearly emphasizes the benefit of using principal values over the isotropic shifts.

As solid shift assignments are often made from comparisons with solution shifts, it is informative to compare the assignments for solid caryophyllene oxide with corresponding solution values. Table 3 lists solution ^{13}C shifts determined from a 2D INADEQUATE analysis. Assigning the solid-state isotropic spectrum with the same relative ordering would result in incorrect assignments for four carbons (i.e. 1, 2, 7 and 9) or 27% of the 15 total carbons. The potential for error is especially evident in carbons 1 and 9. Here the solution and solid-state isotropic spectra have peaks in similar positions and, initially, it might appear that the relative peak order has been preserved in the solid. However, closer examination of the tensor principal values clearly shows that these carbons actually reverse their relative order of isotropic shift in the solid and experience changes of up to 6.6 ppm. In liquids, these differences in principal values are masked by the averaging which gives the isotropic shift. Undoubtedly, such carbons would be misassigned based only on comparison to solution shift values. These changes in the C-1 and C-9 shifts emphasize the value of the *ab initio* tensor comparison methods.

In addition to corrections in the relative order of the peaks, the variations in principal values also provide clear assignments for carbons 14 and 15. The solution INADEQUATE cannot delineate between these diastereotopic carbons as they differ only in their stereochemistry. Multiple solution experiments would be necessary to establish such prochiral assignments. However, as these carbons are readily assigned from the principal values in the solid state, tentative solution assignments may be given (see Table 3) based on comparison with the PHORMAT solid results.

Table 3. Solution and solid-state ^{13}C isotropic shifts for caryophyllene oxide

Carbon	Solution shifts (2D INADEQUATE)	Solid shifts (CP/MAS)[a]
1[b]	50.79	44.2
2[c]	27.23	28.5
3	39.18	38.8
4	59.53	60.0
5	63.53	64.1
6	30.21	32.9
7[c]	29.84	28.1
8	151.71	154.1
9[b]	48.71	50.2
10	39.77	41.9
11	33.97	35.6
12	17.01	18.2
13	112.72	114.1
14	21.66[d]	21.5
15	29.92[d]	30.2

[a] The CP/MAS shifts differ from the $\delta_{average}$ reported in Table 1 by an RMS deviation of ± 0.7 ppm owing to a slight improvement by CP/MAS.
[b,c] Indicate two sets of carbons which have different relative ordering in solution and solid.
[d] Solution assignments tentatively made based on comparison with solid shifts.

Comparison of tensor calculation methods using principal values

Computational details. Before tensor calculation methods can be discussed, a brief description of the methods and abbreviations used is necessary. Both BLYP and BPW91 are density functional methods using Becke's 1988 exchange functional[10] together with the correlation functional of either Lee *et al.*[11] for BLYP or Perdew and Wang[12] for BPW91. The B3LYP and B3PW91 methods are hybrid methods which include both Hartree–Fock and density functional contributions. The B3LYP and B3PW91 methods both use Becke's three parameter functional[13] with the non-local correlation provided either by Lee *et al.*'s expression in the case B3LYP or Perdew and Wang's expression for B3PW91. The gauge-including atomic orbital method was used in all tensor calculations.[14] All tensors were computed using Gaussian 94 software[15] run on IBM RS6000 computers using parallel processing techniques.

Comparison of computational methods. A number of shift tensor calculation methods are currently available. Evaluations of several of these methods and a variety of basis sets have been published using comparison with experimental isotropic shifts.[16] As the isotropic shift is one third of the trace of the chemical shift tensor, this averaging of principal values may allow canceling errors to give accidentally the correct isotropic

Table 4. Comparison of tensor calculation methods[a]

Method	RMS error		Slope	Intercept	Correlation coefficient
	Principal values	Isotropic shift			
HF	4.3	3.0	−1.1066	205.8311	0.9937
BLYP	3.4	2.1	−0.9888	181.4966	0.9960
BPW91	3.0	1.7	−0.9941	185.5905	0.9972
B3LYP	2.8	1.5	−1.0219	187.4204	0.9975
B3PW91	2.4	1.3	−1.0265	190.6721	0.9981
B3PW91[b]	2.3	1.3	−0.9972	193.4006	0.9983

[a] The structure used for all calculations consisted of x-ray positions for heavy atoms and B3LYP/6–31G** refined hydrogen positions.
[b] Calculated using the 6–31+G (2d, p) basis set. All others values computed with the D95** basis set.

shift. A more rigorous test of the theory lies in comparison with actual principal values from powders or, even better, the complete tensor obtained from single-crystal analysis.[1] Such a comparison using several of the currently available tensor computation methods was performed using the principal values of caryophyllene oxide as test data. Included in the evaluation are Hartree–Fock, density functional and hybrid methods. The comparative results are given in Table 4. The availability of 45 PHORMAT-derived principal values for caryophyllene oxide provides a statistically significant number of shifts for making a reliable comparison of the various theoretical approaches.

Examination of the calculated tensors shows that both density functional and hybrid methods perform better than the less intricate Hartree–Fock approach. The B3PW91 method gave the best fit. For comparisons between methods, the D95** basis was chosen. Use of the larger 6–31+G (2d,p) basis with B3PW91 gave slightly improved results compared with experiment. Overall, the quality of these results is considered representative of general aliphatic hydrocarbons. The limited number of multiply bonded carbons and carbons with directly bonded heteroatoms, however, restricts the reliability of these conclusion for such carbons pending the availability of additional examples.

Isotropic solid-state shifts are included in Table 4 to allow comparison with previous theoretical studies.[16] The marked reduction in isotropic errors for caryophyllene oxide over previous comparisons can be attributed to two factors. First, a correlation of experimental shift *vs.* shielding is used to convert the calculated shielding values into calculated shifts. Traditionally, the theoretical shieldings have been treated as absolute values without systematic errors to obtain computed shifts. The correlation approach better accounts for systematic calculation errors and improves the direct comparison with experimental values. A second improvement in the theoretical tensors results from using x-ray geometries for the heavy atoms in the molecule. Previous analyses have focused on tensors obtained soley from *ab initio* determined geometries.[16] However, crystal packing arrangements are capable of significantly modifying geometry, thus changing the calculated shielding values. In solids the frequent observation of polymorphism emphasizes the need for cautious use of *ab initio* geometries.

While it is desirable to use good experimental x-ray geometries for heavy atoms, access to high-quality hydrogen positions in molecules is usually difficult. Constrained *ab initio* calculations actually appear to provide more accurate proton positions and were used to refine the caryophyllene oxide reported x-ray structure.[17] These corrections in the proton positions were made before tensors were calculated. The B3LYP method with the 6–31G** basis set was used for the refinement as this method has been reported to provide high-quality structures.[16] This approach has also been demonstrated to provide proton positions close to neutron diffraction values in single crystals.[18] A comparison of the improvements due to proton position is shown in the correlation of shift to shielding given in Fig. 5. In caryophyllene oxide, the hydrogen refinement improves the RMS error in the principal values by a factor of 2.3. Clearly, the principal values are a sensitive indicator of proton position.

Electron correlation. Recent work has emphasized that neglect of electron correlation in calculation of the chemical shift tensor can result in large errors.[16] Of the methods compared here, the Hartree–Fock method neglects electron correlation whereas all the density functional and hybrid methods include it in some form. In caryophyllene oxide, inclusion of electron correlation is expected to improve most significantly the calculated tensors for the olefinic carbons (8 and 13). Table 5 shows a comparison of experimental and calculated tensors. While the computed tensors which include electron correlation show a significant improvement, the fit to olefinic carbons still remains noticeably worse than the fit to sp^3 carbons, as shown. This result is understandable as electron correlation becomes much greater in π-bonded systems. While the improved fit to the olefinic carbons is clearly evident in the principal values, it is interesting that a comparable analysis using only isotropic shifts leads to the erroneous conclusion that the Hartree–Fock method provides the best fit. This result again emphasizes the greater significance of principal

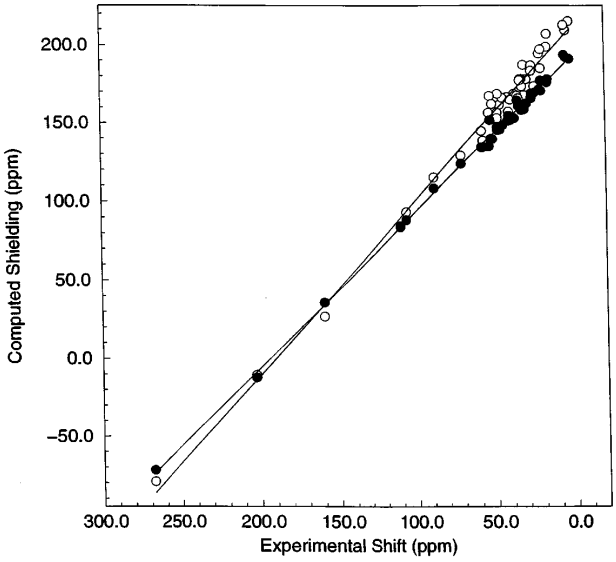

Figure 5. Correlation of shift *vs.* shielding for caryophyllene oxide using the reported x-ray hydrogen positions (○) and with the hydrogen positions refined using the B3LYP/6–31G** *ab initio* calculation (●). Heavy atoms positions are identical in both cases. Without refinement the RMS error is 5.1 ppm with a slope, intercept and correlation coefficient of −1.1159, 212.3890 and 0.9931, respectively. Refinement reduces the RMS error to 2.3 with a slope, intercept and correlation coefficient of −0.9972, 193.4005 and 0.9983, respectively.

shifts over isotropic values in evaluating tensor computational methods. Data from the two olefinic carbons of caryophyllene oxide are still too limited to draw final conclusions; the methods examined appear to require some additional improvements in electron correlation in sp^2 systems.

Tensor calculations based on the GIAO-MP2 method have recently been implemented[16] and appear to provide more accurate tensors in cases where electron correlation is clearly mandated. However, this method is at present available only for fairly small molecules with ≤ 10 non-hydrogen atoms. In the absence of such higher level calculations, the density functional and hybrid methods, used in this work, all appear to give reasonably accurate tensors. For the characterization of many structural and assignment problems, the quality of the density functional or hybrid calculations appears to be sufficient until more advanced theoretical methods can be developed for larger molecules.

Principal value orientations and relationship to structure

In addition to providing comparison data for chemical shift assignments and methodology evaluations, calculated tensors also provide information for orientating principal values with respect to a molecule. This information is not available from the PHORMAT-derived principal values of powder samples. However, tensor principal axis orientations are extremely important as they depend intimately on electronic structure which reflects the variation in the three-dimensional molecular structure. Although calculated orientations cannot be compared directly with PHORMAT data, calculation methods which accurately predict principal values are assumed also to provide reliable orientations. In the case of caryophyllene oxide, the unusually good match between the B3PW91 computed shift values with experimental tensors indicates that the calculated orientations should also be of high quality.

Caryophyllene oxide contains a wide range of carbon types and structural features. To illustrate how principal axis orientations allow shielding to be associated with structural features, the three methyls of caryophyllene oxide will be discussed below in some detail.

Previous analysis has shown that the principal axes of methyl carbons have characteristic orientations with

Table 5. Comparison of experimental and theoretical tensors for sp^2 carbons[a]

Carbon	Principal component	Experiment	HF	BLYP	BPW91	B3LYP	B3PW91	B3PW91[b]
8	11	267.9	277.9	262.6	261.4	265.7	264.7	266.0
	22	159.7	148.7	162.6	161.9	159.2	158.6	158.1
	33	35.4	25.3	24.9	26.3	25.4	26.4	29.2
	Isotropic	154.0	150.6	150.1	149.8	150.1	149.9	151.1
13	11	202.6	217.3	199.2	202.0	204.3	206.4	205.9
	22	88.2	78.5	79.9	85.7	81.2	85.8	85.4
	33	52.4	41.7	42.0	41.7	41.9	41.8	42.0
	Isotropic	114.4	112.5	107.0	109.8	109.2	111.3	111.1
RMSD	Olefin		7.4	6.6	5.4	5.6	4.8	4.2
(principals)	Aliphatic		3.6	3.0	2.4	2.1	1.7	1.8
RMSD	Olefin		2.9	6.0	4.6	4.8	3.8	3.3
(Isotropic)	Aliphatic		3.3	2.3	1.9	1.6	1.3	1.4

[a] The structure used consisted of x-ray positions for heavy atoms and B3LYP/6–31G** refined hydrogen positions.
[b] Calculated using the 6–31 + G (2d, p) basis set. All others values computed with the D95** basis set

respect to the methyl group.[19] Of the three principal axes, δ_{33} invariably lies along or very near to the CH_3—C bond. The other two principal axes are perpendicular to this bond with one component in or near an HCC plane. Here the selected H atom is the methyl hydrogen which is most unique in the local symmetry frame. These axes are designated δ_{CC}, δ_{in} and $\delta_{\perp}$ and are shown in Fig. 6. These designations have the advantage of relating to the three-dimensional molecular structure and hence carry greater chemical information than the serially ordered δ_{11}, δ_{22} and δ_{33} shifts, which can only be related to specific structural moieties using theoretical methods or separated local field experiments.[20]

In caryophyllene oxide, the computed tensors allow the relative ordering of components to be made in terms of δ_{CC}, δ_{in} and $\delta_{\perp}$ as shown in Fig. 7. This ordering shows that the $\delta_{\perp}$ component is represented by δ_{22} in carbons 12 and 14 but by δ_{11} in carbon 15. This ordering clearly demonstrates that the largest variations occur in the perpendicular component, $\delta_{\perp}$, to the specified HCC plane. The δ_{in} and δ_{CC} values exhibit smaller variations between the three methyl shifts. The $\delta_{\perp}$ component therefore dominates variation in the isotropic shift, consistent with previous observations.[19] Examination of calculated tensors has therefore established that the carbon 15 tensor differs from the C-12 and C-14 tensors.

Insight into methyl tensor variation can be gained by comparing caryophyllene oxide methyl tensors to those of axial and equatorial 1,1-dimethylcyclohexane[19] (tensor ordering also included in Fig. 7), which has two diastereotopic methyls similar to C-14 and C-15 in caryophyllene oxide. Comparison of variation in the $\delta_{\perp}$ component with the type of hydrogen–hydrogen interactions in the different structures (Fig. 8) shows that steric interactions at the methyl group correlate strongly with upfield movement of the $\delta_{\perp}$ component. This is clearly seen in carbons 12 and 14 of caryophyllene oxide, where proximate protons are within 2.15 and 2.31 Å of a methyl proton, respectively. Here the $\delta_{\perp}$ components shift by up to 24.9 ppm relative to C-15, which has no van der Waals proton–proton interactions within 2.35 Å. A corresponding trend is observed in 1,1-dimethylcyclohexane, where the presence of two neighbouring protons at 2.33 Å from the axial methyl moves

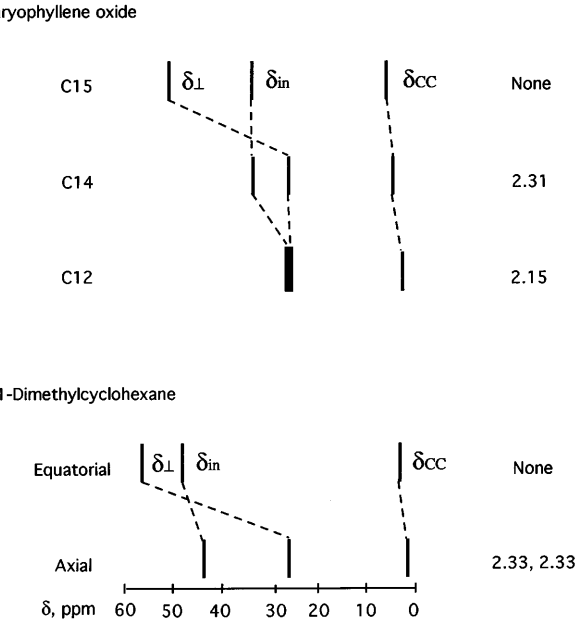

Figure 7. Variation in the principal values associated with specific principal axes in methyl groups. The changes are correlated with sterically unfavorable non-bonded hydrogen interactions (defined here as those interactions where hydrogens are within 2.35 Å of one another). Distances between relevant non-bonded hydrogens are shown on the right side of the figure. The occurrence of similar features in 1,1-dimethylcyclohexane demonstrates that the phenomenon is probably not caused by the unusual electronics associated with the cyclobutane ring but by other factors as outlined.

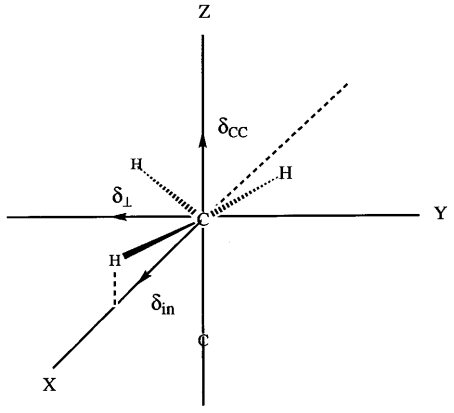

Figure 6. Characteristic orientations of the principal axes in methyl groups. Each of the principal values corresponds to one of these axes, but they can be paired correctly only by using orientational information from computed tensors. Slight variations from the orientations shown arise as local symmetry decreases and are ignored here.

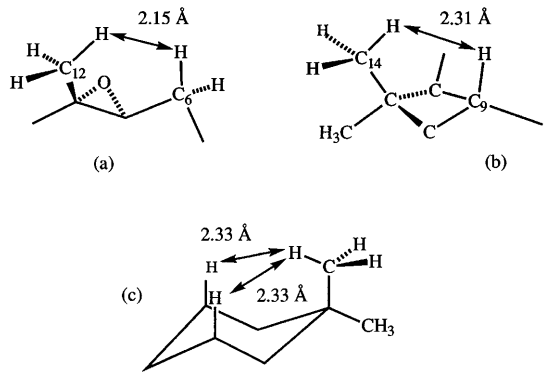

Figure 8. Structural fragments showing unfavorable hydrogen–hydrogen interactions present in the methyl groups of caryophyllene oxide and 1,1-dimethylcyclohexane: (a), (b) and (c) show, respectively, the interactions at C-12 and C-14 of caryophyllene oxide and at the axial methyl of 1,1-dimethylcyclohexane.

the $\delta_\perp$ component 31 ppm upfield relative to the equatorial methyl, which also has no unfavorable proton–proton steric interactions. Indeed, steric interactions at methyls appear to move all principal shift components upfield, but most significantly at the $\delta_\perp$ component. Hence, variations in caryophyllene oxide methyl shifts can be rationalized in terms of sterically perturbed nonbonded hydrogen–hydrogen interactions occurring whenever the interacting protons approach closer than the typical van der Waals distance.

The observation of similar tensor shift features in both four-and six-membered ring systems is strong evidence that the unusual electronics found in cyclobutane rings are not responsible for the variation observed. Other sources for the shift variation such as steric interactions are therefore clearly indicated.

Similar evaluations are possible for other carbons (i.e. CH_2, CH, quaternary and olefinic). Unfortunately, visual correlations, easily seen for the methyl groups, are not as readily apparent, and a more detailed quantitative description involving the non-methyl carbons will be given elsewhere.

EXPERIMENTAL

Caryophyllene oxide was obtained from Aldrich as the pure α-oxide diastereomer and was used as received.

A solution 2D ^{13}C INADEQUATE spectrum of caryophyllene oxide was acquired on a 500 MHz Varian Unity plus spectrometer at 27 °C. The INADEQUATE analysis was performed using a composite pulse sequence designed to provide better coverage of the spectral width.[21] A sample of 220 mg in 0.7 ml of $CDCl_3$ was used for analysis. The spectrum was referenced by assigning the central line of $CDCl_3$ to 77.0 ppm. Data collection was performed using a 16 μs 90° ^{13}C pulse, spectral widths of 19.3 kHz in both dimensions and optimizing the pulse sequence for detection of 55 Hz carbon–carbon coupling constants. A recycle time of 8 s was used and 64 increments were collected with 32 transients each. Total analysis required 9.1 h. Digital resolutions of 301.4 and 0.3 Hz per point were acquired in the F_1 and F_2 dimensions, respectively. Data processing and shift assignments were done in an automated fashion using the software.

A high resolution TPPM decoupled isotropic 1D ^{13}C spectrum was acquired on a Chemagnetics CMX400 spectrometer operating at a carbon frequency of 100.610 MHz. Spectral acquisition was performed with the TOSS sequence[22] at 4 kHz using a 7.5 mm PENCIL probe. Additional run parameters included a 4.6 μs ^1H 90° pulse, a contact time of 3 ms, a recycle time of 2 s, a 15.9 kHz spectral width and a ^1H decoupling frequency of 400.1225 MHz. The Hartmann–Hahn match was set on adamantane. The spectrum was acquired with a digital resolution of 6.4 Hz per point. A TPPM phase-modulation angle of 16° total deviation was used together with a modulation frequency corresponding to a 180°-tip angle. The spectrum was externally referenced to the high-frequency peak of adamantane at 38.4 ppm.

The ^{13}C PHORMAT spectra were collected on a Chemagnetics CMX400 NMR spectrometer using a 30 Hz spinning speed and the previously described PHORMAT pulse sequence.[3] Other acquisition parameters were the same as described for the isotropic spectrum with the addition of a 30 μs echo delay. Spectral widths of 15.9 and 69.9 kHz were used for the isotropic and anisotropic dimensions, respectively. TPPM decoupling was used with a decoupling amplitude corresponding to 54 kHz. For analysis of the olefinic region of the spectrum, the proton decoupler was set to 400.1235 MHz and 20 points were collected with 256 transients per point. Data for the aliphatic region were obtained using a proton decoupling frequency of 400.1225 MHz and 220 points were collected with 64 transients per point. Digital resolutions of the datasets emphasizing olefinic and aliphatic regions were, 797.4 and 72.5 Hz per point respectively, in the evolution dimensions. However, the evolution resolution is essentially irrelevant under TIGER processing as a Fourier transformation is never applied to this dimension. The acquisition dimensions of both spectra were acquired and processed with a digital resolution of 68.3 Hz per point.

Individual powder patterns from the 2D spectrum were provided by TIGER. The TIGER process involves using a high-resolution 1D isotropic spectrum to obtain linewidth and frequency information for each individual resonance. This information is used to construct a linear model which is then applied to the truncated 2D dataset to extract individual powder patterns corresponding to each isotropic shifts. The powder patterns obtained were fitted using the banded matrix approach described elsewhere.[23] The fitted powder patterns have an estimated RMS error in the principal values of $\pm$ 0.7 ppm based on a comparison of the isotropic shift obtained by averaging the fitted principal values with those derived from a high-resolution isotropic spectrum.

CONCLUSION

One of the goals of this study was to establish that TIGER/TPPM improved PHORMAT allows for more routine chemical shift tensor analysis of larger molecules. The success of this approach is most clearly illustrated by the separation of distinct powder patterns for carbons 2 and 7 which differ by only 0.4 ppm in the isotropic dimension in an experiment requiring less than 1 day. Moreover, the quality of the data obtained was not compromised as the close fit to the calculated principal values attests. Overall, 45 ^{13}C principal values were obtained on an unlabeled molecule in this rapid solid-state NMR analysis.

The tensor principal values provided powerful

parameters for assigning shifts and for obtaining solid-state chemical shifts and molecular structure correlations. These data establish the quality of the various computational methods for chemical shift tensors. It is particularly interesting that the calculated olefinic principal values accurately reflect improvements in theoretical methodology whereas the calculated isotropic shifts scramble the ordering. The greater distinction between methods provided by principal values in general demonstrates that tensor principal values offer a superior approach in evaluating tensor computational methods.

Since its introduction, the PHORMAT experiment has been simple to use as it requires little specialized equipment and requires no isotopic labeling.[3] However, these analyses previously have been time consuming. The significant time saving realized by the addition of TIGER and TPPM to PHORMAT now makes these combined methods suitable for routine use.

Steric perturbations of the three methyl carbons in caryophyllene oxide lead to highly correlated structural differences in the chemical shift tensor. This methyl steric study portends a high potential for shift tensors in future chemical structure correlations. With 45 principal values obtainable on caryophyllene oxide, the wealth of tertiary data on this natural product exceeds by a considerable amount most physical chemical measurements. The shift tensor is a tertiary quantity and hence offers a way to make such correlations in a natural manner.

Acknowledgements

Computer resources for tensor computation were provided by the Center for High Performance Computing at the University of Utah. We thank Dr D. W. Alderman for assistance with the use of the banded matrix fitting software and TIGER processing of the PHORMAT data. Funding for this research was provided by NIH grant GM 08521-28.

REFERENCES

1. D. M. Grant, in *Encyclopedia of NMR*, edited by D. M. Grant and R. K. Harris, Vol. 2, pp. 1298–1321. Wiley, Chichester (1996).
2. A. M. Orendt in *Encyclopedia of NMR*, edited by D. M. Grant and R. K. Harris, Vol. 2, pp. 1282–1297. Wiley, Chichester (1996).
3. J. Z. Hu, W. Wang, F. Liu, M. S. Solum, D. W. Alderman, R. J. Pugmire and D. M. Grant, *J. Magn. Reson.* **113**, 210 (1995).
4. G. McGeorge, J. Z. Hu, C. L. Mayne, D. W. Alderman, R. J. Pugmire and D. M. Grant, *J. Magn. Reson.* **129**, 134 (1997).
5. A. E. Bennett, C. M. Rienstra, M. Auger, K. V. Lakshmi and R. G. Griffin, *J. Chem. Phys.* **103**, 6951 (1995).
6. A. M. Orendt, J. Z. Hu, Y.-J. Jiang, J. C. Facelli, W. Wang, R. J. Pugmire, C. Ye and D. M. Grant, *J. Phys. Chem.* **101**, 9169 (1997).
7. K. W. Zilm, in *Encyclopedia of NMR*, edited by D. M. Grant and R. K. Harris, Vol. 7, pp. 4498–4504. Wiley, Chichester (1996).
8. F. Liu, C. Phung, D. W. Alderman and D. M. Grant, *J. Magn. Reson. A* **120**, 231 (1996).
9. D. W. Alderman, M. Sherwood and D. M. Grant, *J. Magn. Reson. A* **101**, 188 (1993).
10. A. D. Becke, *Phys. Rev. A* **38**, 3098 (1988).
11. C. Lee, W. Yang and R. G. Parr, *Phys. Rev. B* **37**, 785 (1988).
12. J. P. Perdew and Y. Wang, *Phys. Rev. B* **45**, 13244 (1992).
13. A. D. Becke, *J. Chem. Phys.* **98**, 5648 (1993).
14. R. Ditchfield, *Mol. Phys.* **27**, 789 (1974).
15. M. J. Frisch, G. W. Trucks, H. B. Schlegel, P. M. W. Gill, B. G. Johnson, M. A. Robb, J. R. Cheeseman, T. A. Keith, G. A. Petersson, J. A. Montgomery, K. Raghavachari, M. L. Al-Laham, V. G. Zakrzewski, J. V. Ortiz, J. B. Foresman, J. Cioslowski, B. B. Stefanov, A. Nanayakkara, M. Challacombe, C. L. Peng, P. Y. Ayala, W. Chen, M. W. Wong, J. L. Andres, E. S, Replogle, R. Gomperts, R. L. Martin, D. J. Fox, J. S. Brinkley, D. J. Defrees, J. Baker, J. P. Stewart, M. Head-Gordon, C. Gonzalez, and J. A. Pople *Gaussian 94* (*Revision A.1*). Gaussian, Pittsburgh, PA (1995).
16. J. R. Cheeseman, G. W. Trucks, T. A. Keith and M. J. Frisch, *J. Chem. Phys.* **104**, 5497 (1996); J. Gauss, *J. Chem. Phys.* **99**, 3629 (1993)
17. Y. A. Gatilov, A. V. Tkachev and Z. V. Dubovenko, *Khim. Prir. Soedin.* **9**, 715 (1982).
18. F. Liu, A. M. Orendt, D. W. Alderman and D. M. Grant, *J. Am. Chem. Soc.* **119**, 8981 (1997).
19. A. Soderquist, J. C. Facelli , W. J. Horton and D. M. Grant, *J. Am Chem. Soc.* **117**. 8441 (1995).
20. J. Z. Hu, D. W. Alderman, R. J. Pugmire and D. M. Grant, *J. Magn. Reson.* **126**, 120 (1997).
21. M. H. Levitt, and R. R. Ernst, *Mol. Phys.* **50**, 1109 (1983).
22. W. T. Dixon, *J. Chem. Phys.* **77**, 1800 (1982).
23. D. W. Alderman, M. S. Solum and D. M. Grant, *J. Chem. Phys.* **84**, 3717 (1986); N. K. Sethi, D. W. Alderman and D. M. Grant, *Mol. Phys.* **71**, 217 (1990).

